ANNALS OF WEST UNIVERSITY OF TIMISOARA PHYSICS
Vol. LXV, 2023

DOI: 10.2478/awutp-2023-0004

UNCERTAINTIES IN CLEAR-SKY SOLAR IRRADIANCE MODELING INDUCED BY THE LIMITED AVAILABILITY OF THE ATMOSPHERIC PARAMETERS

Emil Carstea[1], Marius Paulescu[2,*]

[1]*National Institute of Research and Development for Optoelectronics, Atomistilor 409, 077125, Magurele, Romania*
[2]*Faculty of Physics, West University of Timisoara, V Parvan 4, 300223, Timisoara, Romania*
**Corresponding author: marius.paulescu@e-uvt.ro*

Article Info	Abstract
Received: 1.07.2023 *Accepted: 29.07.2023* **Keywords:** Solar irradiance; Clear-sky; Modeling; Aerosol	In the recent years, great progress has been made in developing terrestrial and satellite-based networks for the measurement of atmospheric parameters, which serve as inputs in clear sky parametric models. However, some parameters may still be missing from the model input due to small temporal sampling or lack of in situ data. This paper presents a case study on the accuracy of the clear-sky solar irradiance estimation by a parametric model, when the availability of inputs is limited. The study was conducted with high-quality radiometric and atmospheric data recorded by the INOE-Magurele station, Romania. Seven different scenarios were studied. In each scenario the clear-sky solar irradiance model was run assuming that certain parameters are missing from the input. The results quantitatively confirm the dominant role of aerosols in establishing the accuracy of solar irradiance estimation under clear sky conditions. The unavailability of the measured Ångström turbidity coefficient may lead to a twofold/threefold increase in the uncertainty of direct-normal/diffuse solar irradiance estimation.

1. Introduction

In the modeling of solar energy at ground level, one of the most important tools is the model for solar irradiance estimation in clear sky conditions. The simplest such models are from the empirical class. Based on data measured in a single location, the empirical clear-sky solar irradiance models are applicable on a limited area around the origin location. Models with applicability over a wider area, even with global coverage, are from the parametric class.

These models estimate solar irradiance on the basis of a number of measured atmospheric parameters, such as the ozone column content, the water vapor column content, the aerosol parameters, etc. Usually, the parametric models are built by weighted averaging of the specific spectral atmospheric transmittances [1]. For a broad discussion related to the accuracy of solar irradiance estimation in clear sky conditions, we point the reader to the comprehensive study [2].

Despite recent progress in the development of terrestrial and satellite-based networks for measuring atmospheric parameters, one or more input parameters of a clear sky parametric model may still not be available. There are several causes that can generate this state of unavailability. The measurements are performed with a temporal sampling much smaller than that required by a particular application. A solution to increase the data granularity is the interpolation (usually linear) between consecutively measured data. Another cause may be the lack of measurements of in-situ atmospheric parameters. In current practice, the solution consists of considering climatological values at the input of the clear sky model. Obviously, all these substitutions of the actual measured atmospheric parameters result in a degradation of the estimates accuracy. For example, when the aerosols are incorrectly represented in a clear-sky solar irradiance model, the relative errors in estimating global solar irradiance may be higher than 20% [3].

This paper reports on a case study of the accuracy in solar irradiance estimation by a parametric model when the inputs availability is limited. The study was conducted as follows. Firstly, a high-quality database, presented in detail in Sec. 2.2, has been established. It contains both radiometric and atmospheric records from the INOE-Magurele station, Romania, briefly introduced in Sec. 2.1. The clear-sky parametric solar irradiance model, denoted PS [4], was run for estimating the direct-normal DNI, global horizontal GHI and diffuse solar irradiance DHI. PS, briefly introduced in Sec. 2.3, requires at input three atmospheric parameters: the ozone column content l_{O3} [cm·atm], water vapor column content w [cm] and the Ångström turbidity coefficient β, as a measure of the atmospheric aerosol loading. Initially, a reference was generated by running the PS model with measured values of the atmospheric parameters to the input. Then, seven scenarios were proposed, in which PS was run assuming that a parameter, two or even all three were missing at the model input. The results are presented in Sec. 3. The accuracy of the estimates in the reference scenario and the other seven scenarios were measured in terms of normalized mean bias errors (*nMBE*) and root mean square error (*nRMSE*). The two statistical indicators are defined in Appendix A. The comparative analysis of the results quantitatively confirms the dominant role of aerosols in establishing the accuracy of solar irradiance estimation under clear sky conditions.

2. Data and Models

2.1. BSRN and AERONET stations at INOE

The Magurele AERONET site is located near the city center, at 6 km southwest of Bucharest, Romania. The AErosol RObotic NETwork (AERONET, http://aeronet.gsfc.nasa.gov) provides a global distribution of long-term AOD observations worldwide. Magurele site contributes to AERONET with sun photometer observations since 2007, and since 2015 operates a sunphotometer/lunar system. The AERONET CIMEL LUNAR system is an automatic triple mode instrument (sun, moon, sky) with double polarization that monitors the optical properties of aerosols, during day and night. The system measures direct solar radiation at nine distinct wavelengths: 340, 380, 440, 500, 670, 870, 936, 1020 and 1640 nm. The aerosol optical depth (AOD), Ångström exponent, fine mode (FMAOD), coarse mode (CMAOD) AOD and fine mode fraction (FMF) are extracted from direct sun measurements using the Beer-Lambert law [5] and ONEILL algorithm [6]. The aerosol microphysical properties are derived from the inversion of the sky radiance measurements ([7]-[9]).

The Solar Radiation Laboratory at Magurele Center for Atmosphere and Radiation Studies (MARS) is located 1.5 km from the Magurele AERONET site. The INO radiation station installed at the Solar Radiation Laboratory is a part of the Baseline Surface Radiation Network (BSRN, https://bsrn.awi.de) and is fully operational since 2019. In 2021, it joined BSRN after a successful evaluation of its quality assurance and quality control (QA/QC) procedures. The quality tests are applied on a daily basis [10]. The radiation station monitors solar radiation, at one second intervals, and includes the following components: the Solys2 solar tracker for tracking the Sun's position, sensors for measuring short-wave downwelling solar radiation: total, diffuse and direct (CMP22 pyranometer, CHP1 pyrheliometer), a sensor for measuring long-wave downward radiation (CGR-4 pyrgeometer), and a CR1000 data-logger. The sensors measure short-wave radiation in the range of 200 to 3600 nm (pyranometer), 200 to 4000 nm (pyrheliometer), and long-wave radiation in the range of 4500 to 42000 nm (pyrgeometer). The pyranometers measure global horizontal irradiance (GHI) and diffuse horizontal solar irradiance (DHI) using a shadowing assembly, and the pyrheliometer measures direct-normal solar irradiance (DNI).

2.2 Joint BSRN – AERONET clear-sky database

Data used in this study are *GHI* and *DHI* stored by INO BSRN station with a resolution of one minute during the following eight clear-sky days from 2021: 15th of January, 26th of February, 3rd of March, 1st of April, 10th of April, 11th of May, 30th of June and 27th of July. The perfect clear sky is visually illustrated in Figure 1, where a beautiful bell shape of the solar irradiance with respect to time can be seen in each of the eight days.

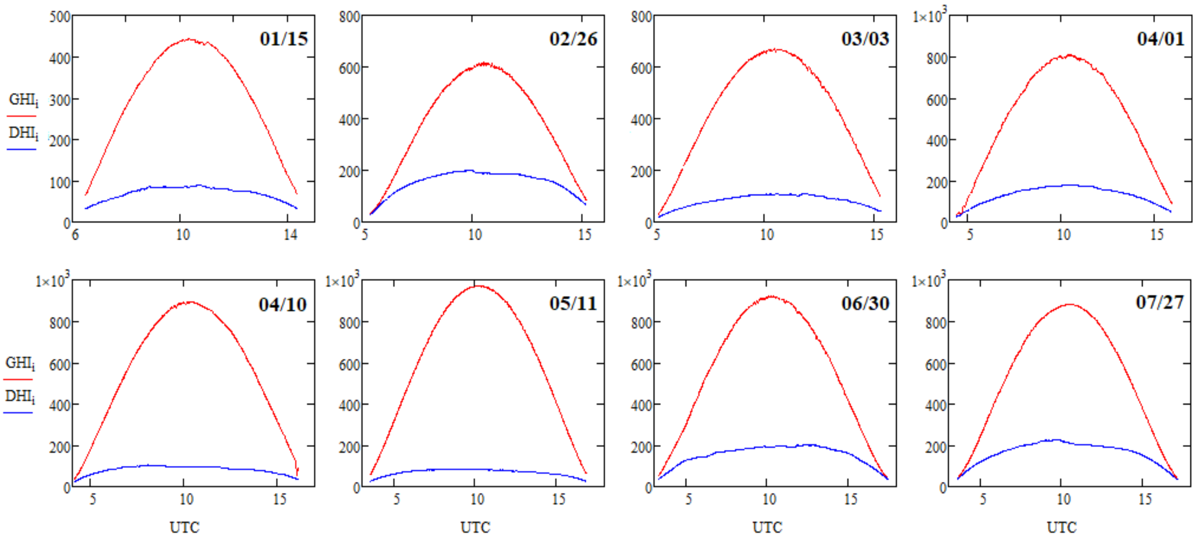

Figure 1. Global horizontal *GHI* [W/m^2] and diffuse *DHI* [W/m^2] solar irradiances recorded during eight clear-sky days from 2021

For the same days, the AERONET L2V3 collected data are: spectral AOD measured at the wavelengths λ: 1020nm, 870nm, 675nm, 500nm, 440nm, 380nm, 340nm, Ångström exponent α, the water vapor column content w [cm], solar zenith angle θ_z [degrees] and the ozone column content l_{O3} (cm·atm). For each line in the database, the Ångström turbidity coefficient β was calculated on the basis of spectral AOD, i.e. $\mathrm{AOD}(\lambda) = \beta\lambda^{-\alpha}$.

Since the BSRN and the AERONET stations measure with different sampling, in the end it was necessary to concatenate the two data files. Only the radiometric data from BSRN, measured simultaneously (that is, the same hour and within the same minute) with those from AERONET were saved. The complete database contains 1262 lines, each line including the time stamp, θ_z, Julian day, GHI, DHI, l_{O3}, w and β.

Table 1 presents a brief statistic of the atmospheric parameters applied at the PS model input. For each parameter, the range of variation is quite wide. The average value of the ozone column content is close to the climatological value, but instants with a substantially thinner/thicker ozone layer were also recorded. The water vapor column content shows a similar statistic. The solar irradiance data were recorded during periods with small atmospheric turbidity but also in episodes with significant atmospheric aerosol loading (β > 0.2). The values of the Ångström exponent show the expected industrial-urban aerosol and the presence of dust during the aerosol pollution episodes. To generate a clearer picture of the inputs in the PS model, the distribution of each atmospheric parameter is presented in Fig. 2.

Table 1. Statistics of the atmospheric parameters included in the database: ozone column content l_{O3} (cm·atm). water vapor column content w [cm], the Ångström turbidity coefficient β and the Ångström exponent α.

Parameter	l_{O3} [cm·atm]	w [cm]	β	α
Min	0.323	0.49	0.024	0.282
Max	0.374	3.30	0.272	1.742
Mean	0.354	1.51	0.124	1.035
SD	0.019	1.02	0.082	0.358

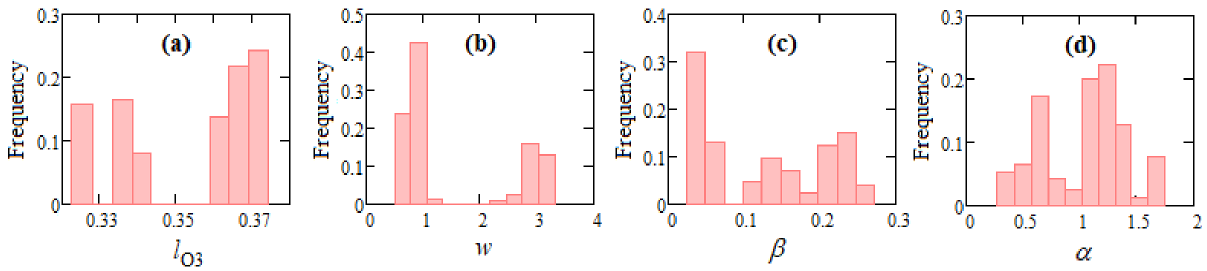

Figure 2. Distributions of the atmospheric parameters included in the database: ozone column content l_{O3} (cm·atm), water vapor column content w [cm], the Ångström turbidity coefficient β and the Ångström exponent α

2.3 Clear-sky solar irradiance model

The influence of the atmospheric parameters' availability on the accuracy of clear-sky solar irradiance estimates was studied using the PS model [4]. This is a very simple model which estimates the atmospheric transmittance based on five attenuators: ozone, water vapor and mixed gases absorption, and Rayleigh and aerosol scattering. The specific atmospheric transmittances are expressed with the equation:

$$\bar{\tau}_l(x_l) = \exp\left[-x_l\left(a + bx_l + cx_l^{-d}\right)\right]. \quad (1)$$

The empirical coefficients for all the five atmospheric attenuators are listed in Table B1, from Appendix B.

The equations for the direct-normal and diffuse solar irradiances in the PS model are as follows:

$$G_n = G_{SC}\varepsilon_j \overline{\tau}_{O3}\overline{\tau}_w \overline{\tau}_g \overline{\tau}_R \overline{\tau}_a \quad (2)$$

$$G_d = \gamma G_{SC}\varepsilon_j \overline{\tau}_{O3}\overline{\tau}_w \overline{\tau}_g (1-\overline{\tau}_R \overline{\tau}_a)\cos\theta_z \quad (3)$$

PS assumes the downward fraction γ as an empirical parameter. For the station Timisoara, Romania (45°46'N, 21°25'E, 86m a.s.l.), Ref. [4] reports the value $\gamma = 0.432$. Over time, the performance of the PS model was evaluated in many places around the world by different studies focused on clear-sky solar irradiance (e.g., [11]), showing a reasonable accuracy.

3. Results and discussions

PS model was run assuming the scenarios summarized in Table 2. In the first scenario (reference), it is assumed that all parameters at the input of the PS model are known. In the other seven scenarios from Table 2, one or more input parameters are assumed to be unknown, and they are replaced with average values.

Table 2. Definitions of scenarios. The input parameters of the PS models (ozone column content l_{O3} (cm·atm). water vapor column content w [cm], the Ångström turbidity coefficient β) are assumed to be measured "M" or averaged "-".

Scenario	1	2	3	4	5	6	7	8
l_{O3}	M	-	M	M	-	-	M	-
w	M	M	-	M	-	M	-	-
β	M	M	M	-	M	-	-	-

Figure 3 presents in terms of *nMBE* and *nRMSE*, the accuracy of DNI, DHI and GHI estimates in the reference scenario and the other seven scenarios. Looking at the reference scenario, at the INOE-Magurele station, PS underestimates DNI (*nMBE* = -0.128) and GHI (*nMBE* = -0.105) while DHI estimates are not biased. The same accuracy (around *nRMSE* = 0.13) is observed when estimating any of the three components. Replacing the values of the ozone column content and water vapor column content (scenarios 2,3 and 5) with average values does not significantly change the estimation accuracy of any of the solar irradiance components.

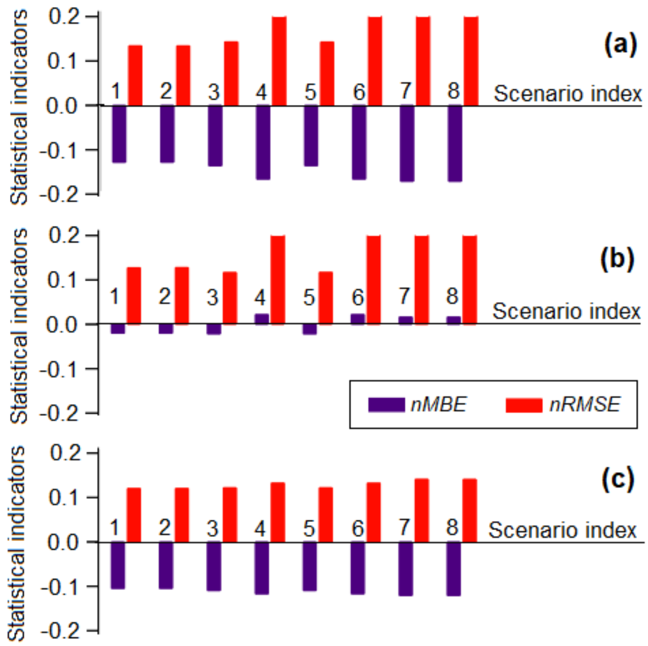

Figure 3. Statistical indicators of PS accuracy in estimating: (a) DNI, (b) DHI and (c) GHI. PS was run in the scenarios from Table 2

The situation is completely different in the case of aerosols. The unavailability of the measured Ångström turbidity coefficient (scenario 4) leads to a twofold increase in *nRMSE* (from 0.124 to 0.24) in the case of DNI and a threefold increase in *nRMSE* (from 0.127 to 0.357) in the case of DHI. When the Ångström turbidity coefficient is replaced by the average value, even in the most unfavorable case (scenario 8), the accuracy of DNI and GHI estimates remains around the two values reached in scenario 4. The behavior of PS in GHI estimation is different and somehow strange. Visual inspection of Figure 3c shows that as PS is applied in increasingly worse scenarios, the accuracy in GHI estimation decreases, but much more slowly than in the case of the other two components. The lowest accuracy is recorded in scenario 8 (*nRMSE* = 0.141), representing a 17.5% decrease compared to the reference scenario, when PS achieves the best accuracy in GHI estimation (n*RMSE* = 0.120). This behavior is explained by the biases of the two components: DNI and DHI. While DNI is increasingly underestimated, DHI ends up being overestimated in the worst scenario. In other words, the errors in the estimation of DNI and DHI compensate for each other.

4. Conclusions

This paper summarizes the results of a case study on the accuracy of the clear-sky solar irradiance estimation by a parametric model, when the availability of inputs is limited. The PS [4] clear-sky parametric solar irradiance model was run for estimating DNI, DHI and

GHI. The study was conducted with high-quality radiometric and atmospheric data recorded by the INOE-Magurele station, Romania. The results quantitatively confirm the dominant role of aerosols in establishing the accuracy of solar irradiance estimation under clear sky conditions. The unavailability of the measured Ångström turbidity coefficient may lead to a twofold/threefold increase in the uncertainty of DNI/DHI estimation. Even if this case study is limited to a solar irradiance model and data from a single location, the results highlight unequivocally that an inadequate knowledge of aerosol parameters can lead to large errors in the estimation of solar irradiance components.

Acknowledgments

E. Carstea acknowledges the support of MCID, through the Core Program within the National Research Development and Innovation Plan 2022-2027, project no. PN 23 05.

Appendix

A. Statistical indicators of accuracy

The estimation accuracy is quantified in terms of two common statistical indicators very often used in solar radiation modeling, i.e. normalized root mean square error (*nRMSE*) and normalized mean bias error (*nMBE*):

$$nRMSE = \frac{\left[M \sum_{i=1}^{M} (c_i - m_i)^2 \right]^{1/2}}{\sum_{i=1}^{M} m_i} \tag{A1}$$

$$nMBE = \frac{\sum_{i=1}^{M} \left(c_i - m_i \right)}{\sum_{i=1}^{M} m_i} \tag{A2}$$

where c and m refer to estimated and measured values, respectively, while M denotes the number of measurements.

B. Empirical coefficients in the PS atmospheric transmittance

Table B1 The variable x_l and the coefficients a, b, c and d from Eq. (1) for the specific atmospheric transmittances in the PS model.

$\bar{\tau}_l$	x_l	*a*	*b*	*c*	*d*
$\bar{\tau}_{O3}$	$m \cdot l_{O3}$	0.0184	-0.0004	0.022	-0.66
$\bar{\tau}_w$	$m \cdot l_w$	-0.002	$1.67 \cdot 10^{-5}$	0.094	-0.693
$\bar{\tau}_g$	m	-5.410^{-5}	$-3.8 \cdot 10^{-6}$	0.0099	-0.62
$\bar{\tau}_R$	m	0.709	0.0013	-0.5856	0.058
$\bar{\tau}_a$	$m \cdot \beta$	1.053	-0.083	0.3345	-0.668

References

[1] José A. Ruiz-Arias, Spectral integration of clear-sky atmospheric transmittance: Review and worldwide performance, Renewable and Sustainable Energy Reviews, Volume 161, 2022, 112302. [2]

[2] Xixi Sun, Jamie M. Bright, Christian A. Gueymard, Xinyu Bai, Brendan Acord, Peng Wang, Worldwide performance assessment of 95 direct and diffuse clear-sky irradiance models using principal component analysis, Renewable and Sustainable Energy Reviews, Volume 135, 2021, 110087,

[3] Calinoiu D, Stefu N, Paulescu M, Trif-Tordai G, Mares O, Paulescu E, Boata R, Pop N, Pacurar A. Evaluation of errors made in solar irradiance estimation due to averaging the Angstrom turbidity coefficient. Atmospheric Research 2014; 150: 69-78.

[4] Paulescu, M., Schlett, Z., "A simplified but accurate spectral solar irradiance model," Theor. Appl. Climatol. 75, 203-12 (2003)

[5] Holben BN, Tanre D, Smirnov A, Eck TF, Slutsker I, Abuhassan N, Newcomb WW, Schafer JS, Chatenet B, Lavenu F, Kaufman YJ, Castle JV, Setzer A, Markham B, Clark D, Frouin R, Halthore R, Karneli A, O'Neill NT, Pietras C, Pinker RT, Voss K, Zibordi G (2001) An emerging ground-based aerosol climatology: aerosol op- tical depth from AERONET. J Geophys Res 106(D11):12,067–12, 097. https://doi.org/10.1029/2001JD900014

[6] O'Neill NT, Eck TF, Smirnov A, Holben BN, Thulasiraman S (2003) Spectral discrimination of coarse and fine mode optical depth. J Geophys Res 108(4559):393. https://doi.org/10.1029/ 2002JD002975

[7] Dubovik O, King MD (2000) A flexible inversion algorithm for retrieval of aerosol optical properties from sun and sky radiance measure- ments. J Geophys Res 311(105):20,673–20,696. https://doi.org/10. 1029/2000JD900282

[8] Dubovik O, Sinyuk A, Lapyonok T, Holben BN, Mishchenko M, Yang P, Eck TF, Volten H, Noz OM, Veihelmann B, van der Zande WJ, Leon J, Sorokin M, Slutsker I (2006) Application of spheroid models to account for aerosol particle nonsphericity in remote sensing of desert dust. J Geophys Res 111:D11,208. https://doi.org/10.1029/ 2005JD006619

[9] Holben BN, Eck TF, Slutsker I, Smirnov A, Sinyuk A, Schafer J, Giles D, Dubovik O (2006) Aeronet's Version 2.0 quality assurance criteria. Proc. SPIE Remote Sens. Atmos. Clouds 6408:64080Q. https://doi. org/10.1117/12.706524

[10] Long, C. N. and Dutton, E. G., 2022: BSRN Global Network recommended QC test, Version 2.0. Accessed from bsrn.avi.de.

[11] Calinoiu, D., Stefu, N., Boata, R., Blaga, R., Pop, N., Paulescu, E., Sabadus, A., Paulescu, M., "Parametric modeling: A simple and versatile route to solar irradiance," Energ. Convers. Manage. 164, 175-187 (2018). DOI:10.1016/j.enconman.2018.02.077